COMPREHENSIVE STUDY OF UNSTEADY PRESSURE PULSATIONS INDUCED BY THE SPIRAL VORTEX STRUCTURE IN A CONICAL DIFFUSER

David ŠTEFAN*

V. Kaplan Department of Fluid Engineering, Brno University of Technology, Czech Republic

Pavel RUDOLF

V. Kaplan Department of Fluid Engineering, Brno University of Technology, Czech Republic

Martin HUDEC

V. Kaplan Department of Fluid Engineering, Brno University of Technology, Czech Republic

Vladimír HABÁN

V. Kaplan Department of Fluid Engineering, Brno University of Technology, Czech Republic

ABSTRACT

The decelerated swirling flow often breaks down into helical structure which is unstable and causes unsteady velocity and pressure fields. The numerical and experimental investigation of this flow pattern is carried out on the experimental apparatus consisting of the swirl generator (source of strong swirling flow) and the conical diffuser (equipped with the series of pressure transducers). The experimental measurements are focused on complex pressure measurements in order to distinguish between synchronous and asynchronous pulsations induced by the vortex structure and examine their changes in relation to the flow rate. The numerical simulations are carried out to visualize vortex shape and compare computed pressure fields with the experimental ones. The open source CFD software OpenFOAM employing realizable k-ε turbulence model is used for the numerical simulations. Agreements between numerical end experimental results are discussed.

KEYWORDS

swirling flow, pressure pulsations, diffuser, spiral vortex, OpenFOAM

1. INTRODUCTION

In many cases of industrial fluid flows the flow instability called vortex breakdown occurs as a consequence of instability mechanisms in decelerated swirling flow. The vortex breakdown can be found in several forms related to the character of particular flow. Nevertheless, many forms of the vortex breakdown are not relevant to the industrial applications, e.g. bubble form

* *Corresponding author:* V. Kaplan Department of Fluid Engineering, Faculty of Mechanical Engineering, Brno University of Technology, Technická 2896/2, 616 69 Brno, Czech Republic, phone: +420 54114 2341, email: david.steffan@gmail.com

of vortex breakdown in low-Re flows [1]. In case of hydraulic turbines with constant pitch of the runner (e.g. Francis turbine), the high Reynolds number spiral form of the vortex breakdown (called vortex rope) appears, when the turbine is operated at part load, see Fig.1.

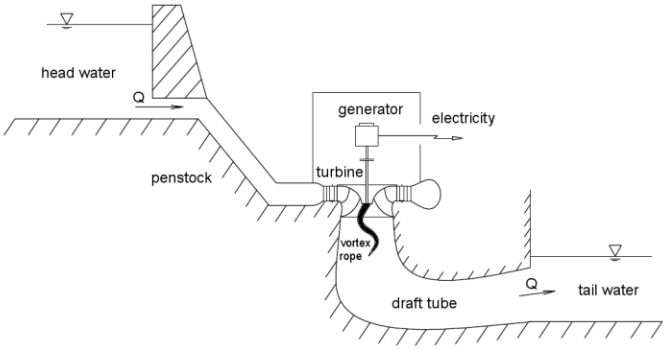

Fig.1 Vortex rope in the drfat tube of hydrailic turbine

The mechanism of the spiral breakdown is described as a rapid axial deceleration towards what appears to be a stagnation point. Then the straight swirl expands outwards into helix and after one or two windings of the spiral, the filament breaks up into large scale unsteadiness and turbulence [1]. The spiral is the basic form of the breakdown [3].

Despite the large database [4], covering investigations of the vortex breakdown during the last forty five years and extensive theoretical, experimental and computational research, we still lack deeper understanding of all influences on origin of this phenomena and their relations to the vortex rope properties (frequency of the precessing motion, helix shape, pressure amplitudes, etc.) [5]. Some important features of the vortex breakdown related to the flow in the draft tube can be mentioned - the vortex breakdown is asymmetric and time dependent, precessing vortex core is developed and laid in the mixing layer of vortex sheet form in between the main flow and recirculation region [4]. The spiral form of the vortex breakdown can be interpreted as a nonlinear global mode originating at the convective/absolute instability transition point of the axisymmetrical vortex breakdown bubble [6], [7]. Susan-Resiga et al. [8] concluded that the most significant case of the vortex breakdown in conical diffusers is a high Re spiral shape with central quasi stagnant region.

In present study the simplified apparatus of swirl generator consisting of ten stationary blades designed so that the fully axial flow is converted into flow with significant tangential component was used in order to obtain the spiral form of the vortex breakdown. The blades are situated on the inner spike which acts as a hub. The trailing edge deflection from the axial direction is 30 degrees at spike side and linearly changes to 50 degrees on outer wall (shroud). The blade length is 40 mm and blade thickness is 1 mm. Consequently the swirling flow is decelerated in the conical diffuser where the spiral vortex breakdown appears in a form of vortex structure. The main swirl generator dimensions are presented in Fig.2.

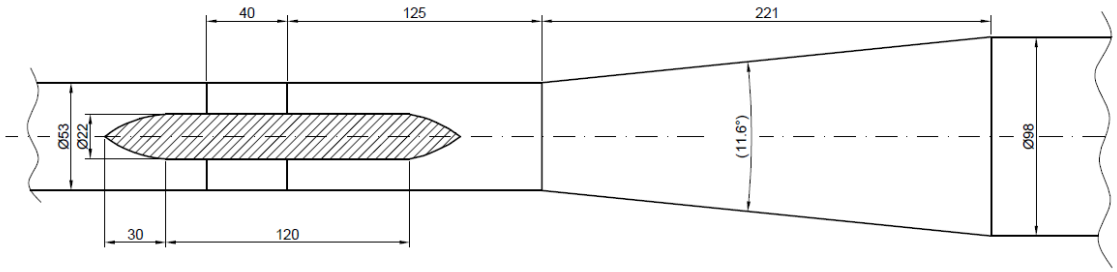

Fig.2 Dimensions of swirl generator apparatus

2. EXPERIMENTAL MEASUREMENTS

The experimental measurements were performed employing the hydraulic circuit with the gravity driven flow, where the constant head was maintained. The main geometrical features of test rig and location of the swirl generator apparatus are shown in Fig.3.

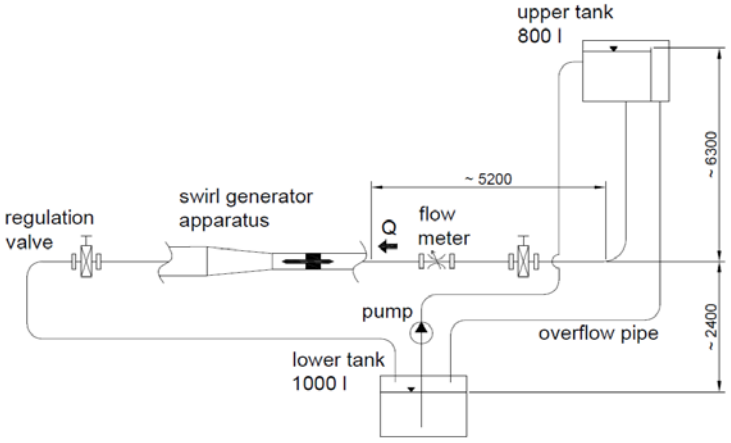

Fig.3 Scheme of experimental test rig

The unsteady pressure pulsations are measured in seven locations p0 – p6. The first pressure sensor p0 is situated 591 mm in front of the cone inlet, the five pressure sensors are situated in the diffuser part (sensor p1 is situated 20 mm in front of the cone and p2 – p5 are situated in the cone) and sensor p6 is situated 291 mm downstream at the outlet of the diffuser. In order to distinguish between synchronous and asynchronous pulsations the oppositely oriented pressure sensors p1* - p5* are included, see Fig.4.

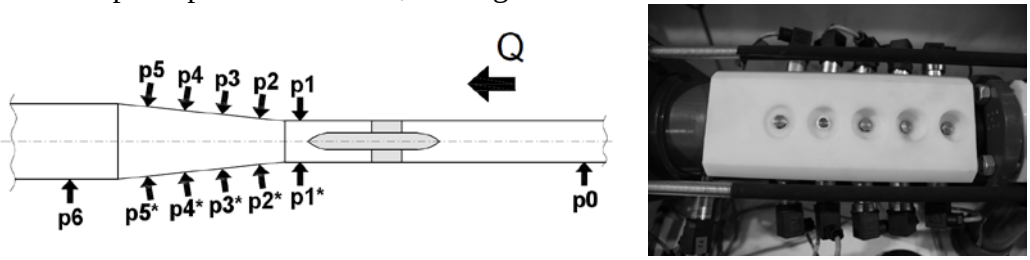

Fig.4 The pressure sensors arrangement (left) of experimental measurements (right)

The dimensionless sensor locations are calculated and measuring cross-sections s1 – s5 are defined with respect to inlet diameter D = 0.0536 m, see Tab.1.

Sensor pairs	Location L/D (1)
p0	-11.026
s1 - p1/p1*	-0.3731
s2 - p2/p2*	0.6269
s3 - p3/p3*	1.5485
s4 - p4/p4*	2.4720
s5 - p5/p5*	3.3955
p6	5.4291

Tab.1 Pressure sensor locations

2.1 Time evolution of the spiral vortex

The transparent diffuser is utilized in order to visually capture the cavitating vortex using the high speed camera recording. The precessing vortex rolls up and decays periodically

generating the synchronous pressure pulsations. One period of the vortex decay is captured in series of images presented in Fig.5.

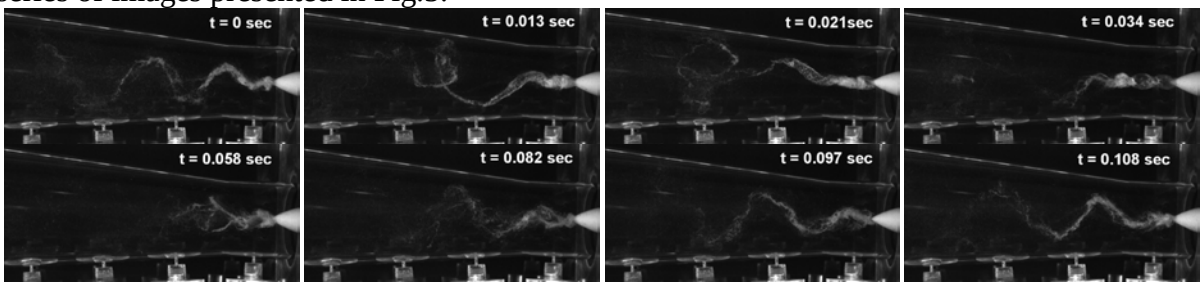

Fig.5 The experimental observation of the spiral vortex time evolution

2.2 Decomposition of pressure signal to the asynchronous and synchronous pulsations

The measured static pressure signal is decomposed to the synchronous (longitudinal) pulsations

$$p_{synch} = \frac{p_i + p_i^*}{2} \quad (1)$$

and to the asynchronous (transverse) pulsations

$$p_{asynch} = \frac{p_i - p_i^*}{2} \quad (2)$$

where the index number $i = 1 - 5$ refers sensors order in the flow direction. The dominant amplitude of asynchronous pressure pulsations was found for the first four measuring cross-sections s1 – s4. One can see in Fig.6 (right) that for the particular flow rates the magnitude of asynchronous pulsations frequency decreases downstream of the diffuser.

The synchronous pressure pulsations are realized in a longitudinal direction. According to section 2.1 the longitudinal instability of the vortex structure related to the spiral decay is a source of strong synchronous pulsations realized alongside of the first three cross-sections, see Fig.6 (right). The frequencies should remain unchanged through the investigated cross-sections at particular flow rate. One can see that this assumption is proved with slight discrepancies due to the complex vortex behavior. For flow rates lower than Q < 4 l/s it was already not possible to clearly distinguish dominant amplitude of synchronous frequency.

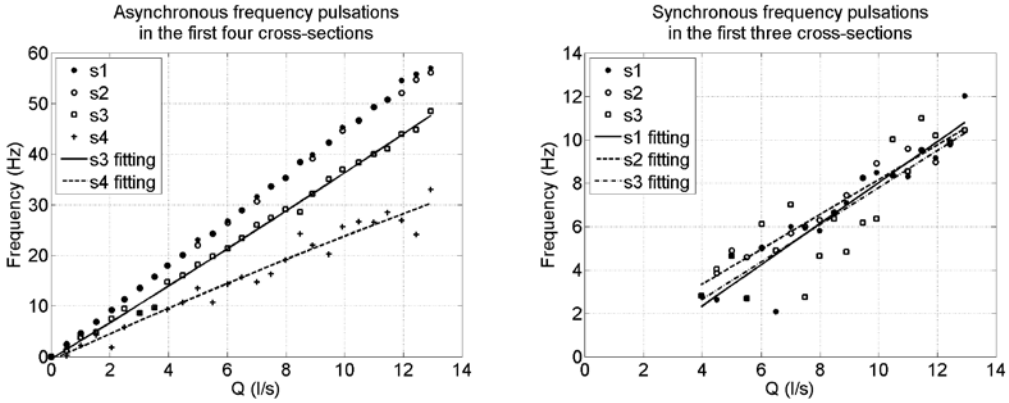

Fig.6 Asynchronous (left) and synchronous (right) pressure pulsations

2.3 Asynchronous frequency decrease alongside of the diffuser

In section 2.1 is shown that the spiral vortex decays and rolls up periodically. From closer visual observation of image ensemble it was found that the upstream part of the vortex rotates faster than the downstream part. Consequently the vortex spiral turns into the loop and collapses upstream in form of straight short vortex (see t = 0.013 – 0.034 sec in Fig.5.). While

the frequency magnitudes of asynchronous pulsations are equal in the first and second cross-sections, the frequency magnitudes decrease in the third and fourth cross-section. Two reasons of asynchronous frequency decrease downstream of the diffuser are assumed 1.) diameter differences respectively differences in the circumference of particular investigated cross-sections and 2.) vortex collapse upstream to the diffuser.

According to the first assumption the frequencies in the third and fourth cross-sections are treated from the increasing diameter ratio of the diffuser opening. Considering the diameter of the second cross-section D_2 = 0.05973 as an initial one and diameter D_k related to the k-th cross-section the ratio of the diameter growth defined as D_k/D_2 can be computed, see Tab. 2.

Cross – section	Diameter (m)	D_k/D_1 (1)
s2	0.05973	1
s3	0.07	1.17194
s4	0.08	1.33936

Tab.2 Diameter growth ratio.

This ratio is then used to increase (i.e. "correct") frequency magnitudes in the third and fourth cross-sections, thus the new value of frequency in the third cross-section is defined as $f_3^* = f_3 \,.\, D_2/D_1$.

The evolution of these treated frequencies against the flow rate is plotted in Fig.7 (left). One can see that while for the third cross-section the agreement with upstream cross-sections s1 and s2 is achieved, for the fourth cross-section the values of frequencies are still lower.

The collapsing spiral form of the vortex is consequence of significant synchronous pulsations. As was shown in section 2.2 the synchronous pressure pulsations are realized mainly in the first three cross-sections. Consequently the synchronous frequency portion is added to the fourth cross-sections deprived from the synchronous pulsations when the spiral vortex collapses upstream to the diffuser. One can see in Fig.7 (right) that the frequencies for full range of flow rates in the fourth cross-section now fits very well with ones in the upstream cross-sections.

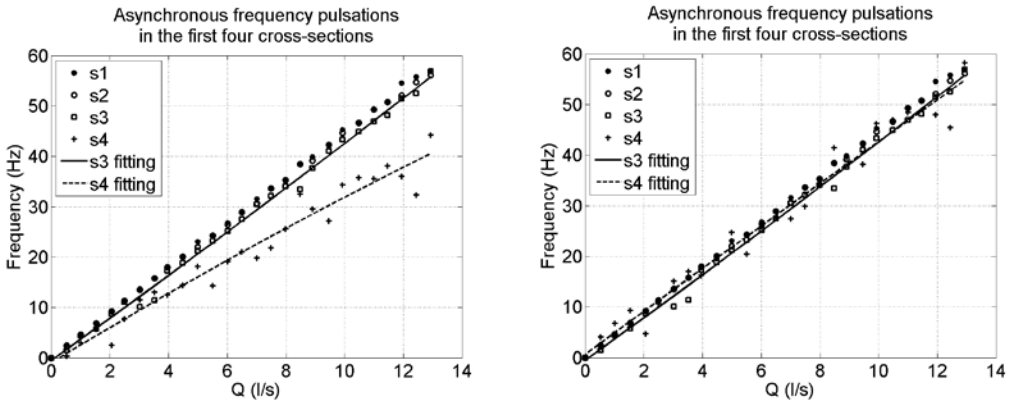

Fig.7 The frequency values of asynchronous pressure pulsations in the third and the fourth cross-sections treated by diameter growth ratio (left) and in the fourth cross-sections treated by influence of synchronous pulsations (right)

3. CFD COMPUTATIONS

The numerical simulation is carried out using open-source code OpenFOAM (OF) in version 2.2.2. The unsteady calculations employing the large time-step solver `PIMPLE` (merged PISO and SIMPLE algorithm) together with realizable k-ε turbulence model are carried out

with prescribed boundary conditions of the constant velocity at the inlet patch and constant pressure $^{p}/_{\rho} = 0$ at the outlet patch. The turbulent kinetic energy k and turbulent dissipation rate ε were computed considering 5% of turbulence intensity at the inlet boundary.
The computational grid was built in the software Gambit and then converted into OpenFOAM format. The computational domain is shown in Fig.8. Two kinds of elements are used. While the major part of the domain contains hexahedral elements the tetrahedral elements are used in order to treat regions of sharp spikes. Whole mesh consists of 3 967 877 elements. The numerically computed velocity fields were previously compared with LDA measurements with acceptable agreement.

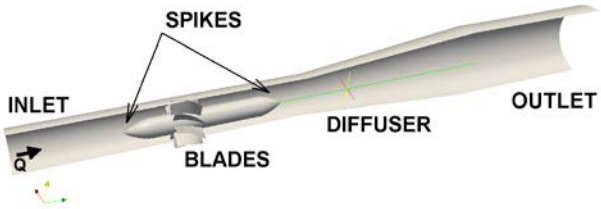

Fig.8 Computational domain

3.1 Temporal evolution of computed vortex shape

The time-evolution of numerically computed vortex structure (represented as the iso-contour of low static pressure) is shown in Fig.9. It has to be noted that while the experimental observation is presented for flow rate Q = 13.5 l/s (due to the strongest cavitation well visualizing the vortex core) the numerical results presented below are for flow rate Q = 7 l/s and no cavitation. Nevertheless comparing the Fig.9 with Fig.5 it is clear that the numerically computed collapse of the spiral vortex is well correlated with the experimental one.

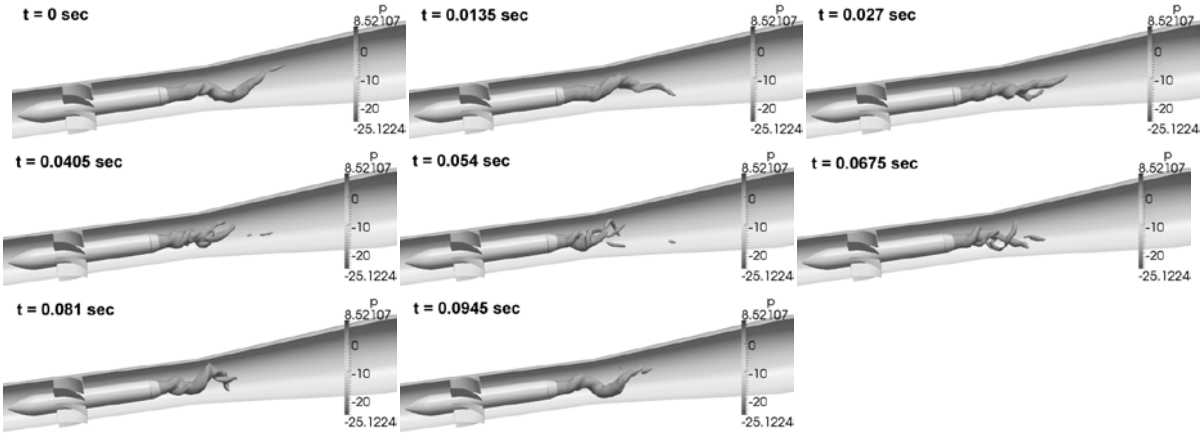

Fig.9 Numerical calculated time evolution of the vortex structure

4. COMPARISON OF EXPERIMENTAL AND NUMERICAL RESULTS

In Fig.10 the comparison of pressure recovery $c_p = \frac{p_{s(i)} - p_{s(1)}}{\frac{1}{2}\rho \bar{v}_1^2}$ is carried out between numerical and experimental results. The best agreement is obtained for flow rate Q = 7 l/s. On the other hand largest discrepancy is for the flow rate Q = 5 l/s where the computed pressure recovery underestimates experimental values in all sensor locations. For both higher investigated flow rates Q = 11 and 13 l/s the numerical pressure recovery overestimates the numerical one especially in sensor location situated at L/D = 0.6269 where the largest amplitudes appear.
The numerically computed and experimentally measured frequencies of asynchronous pressure pulsations are compared in Fig.11 for the first four sensor locations. Similarly to the

pressure recovery the best agreement is obtained for flow rate Q = 7 l/s. Both the magnitude of asynchronous pressure pulsations and decreasing tendency downstream of the diffuser are well predicted. On the other hand the largest discrepancy can be found at flow rate Q = 11 l/s.

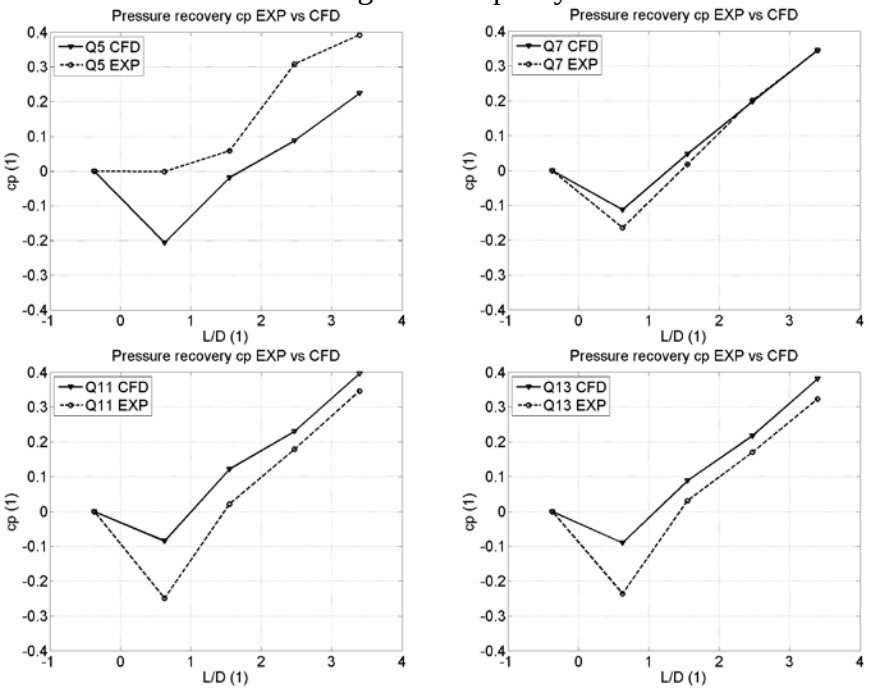

Fig.10 Pressure recovery factor experiment (EXP) vs. calculation (CFD)

While the frequency magnitudes are overestimated for the first two locations of pressure sensors the large underestimation is obtained for the third and fourth sensor location. Well predicted results are also for flow rates Q = 5 l/s and 13 l/s. Nevertheless underestimation of experimentally obtained asynchronous frequency can be found for the third and fourth sensor location at flow rate Q = 5 l/s.

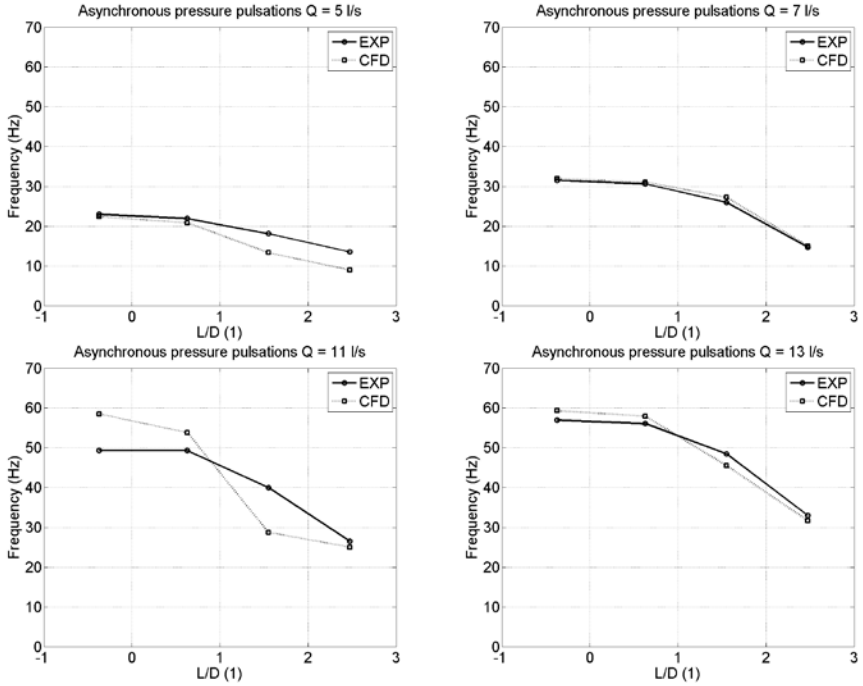

Fig.11 Frequency of asynchronous pressure pulsations (EXP) vs. calculation (CFD)

5. CONCLUSION

The steady and unsteady pressure fields were compared. It was shown that really good agreement between numerical and experimental results can be found. The experimentally observed strong unsteady vortex behaviour is well captured by the numerical calculation. The single phase calculation (i.e. omitting the effect of cavitation) is considered as the main source of result discrepancy.
It was shown that the periodically decaying vortex structure decreases the magnitude of asynchronous pressure pulsations downstream of the diffuser. This phenomenon was observed both experimentally and in numerical simulation.

6. ACKNOWLEDGEMENTS

Research was supported by project FSI-S-14-2480 (Innovative fluid machines) of Brno University of Technology, Faculty of Mechanical Engineering.

7. REFERENCES

[1] Rudolf, P.: Simulation of vortex breakdown in an enclosed cylinder as a preliminary study of the draft tube vortex rope creation, FMA'08: Proc. 6th IASME/WSEAS Int. Conf. on Fluid Mech. and Aerodyn.: Book Series: WSEAS Mech. Eng. Series, pp.147-151, 2008

[2] Novak, F.G.: *An Experimental Investigation of Vortex Breakdown in Tubes at High Reynolds Numbers*. Dissertation thesis. (Naval Postgraduate School. Monterey, California 1998).

[3] Brücker, C.: Study of Vortex Breakdown by Particle Tracking Velocimetry (PTV) Part 2: Spiral-Type Vortex Breakdown. *Exp. in Fluid.* Vol. 14. 1993. pp. 133-139.

[4] Lucca-Negro, O., O'Doherty, T.: Vortex breakdown: a review, in: *Annual Review of Fluid Mechanics.* Vol. 10. 2001. pp. 221-246.

[5] Rudolf, P.: Connection between inlet velocity field and diffuser flow instability, in: *Applied and Computational Mechanics.* Vol. 3, No. 1. 2009. pp. 177 – 184.

[6] Gallaire, F., Ruith, M., Meiburg, E., Chomaz, J.-M., and Huerre, P.: Spiral Vortex Breakdown as a Global Mode. *J. Fluid Mech*. Vol. 549. 2006. pp. 71–80.

[7] Zhang, R.-K., Cai, Q.-D., Wu, J.-Z., Wu, Y.-L., Liu, S.-H., and Zhang, L.: The Physical Origin of Severe Low-Frequency Pressure Fluctuations in Giant Francis Turbines," *Mod. Phys. Lett. B*, Vol. 19. 2005. pp. 99–102.

[8] Susan-Resiga, R.F., Muntean, S., Hasmatuchi, H., Anton, I., Avellan, F.: Analysis and Prevention of Vortex Breakdown in the Simplified Discharge Cone of a Francis Turbine. *Journal of Fluids Engineering*. 2010. Vol. 132.

[9] Štefan, D., Zubík, P., Hudec, M., Habán, L. Numerical and experimental investigation of swirling flow in a conical diffuser. 2015. *EPJ Web of Conferences*. Vol. 92.